FAILURE MECHANISMS AND BEARING CAPACITY OF STRIP FOOTINGS ON SAND OVER CLAY UNDER CENTRIC AND ECCENTRIC LOADING

Pham Ngoc Quang[1]*, Pham Ngoc Vinh[1], Huynh Ngoc Thi[2,3], Doan Hoang Tai[4], Vu Thi Hanh[1]

[1]The University of Danang - University of Science and Technology, Vietnam
[2]Ho Chi Minh City University of Technology (HCMUT) – VNU - HCM, Vietnam
[3]Vietnam National University Ho Chi Minh City, Vietnam
[4]Hue University – Quang Tri Branch, Quang Tri Province, Vietnam

*Corresponding author: pnquang@dut.udn.vn

(Received: December 31, 2025; Revised: March 09, 2026; Accepted: March 25, 2026)

DOI: 10.31130/ud-jst.2026.24(3).737E

Abstract – The bearing capacity and failure behavior of strip footings on two-layered soils are examined under concentric and eccentric loading using the Rigid Plastic Finite Element Method (RPFEM). The soil system consists of a sand layer overlying weak clay. A parametric study evaluates the effects of sand thickness D, internal friction angle ϕ, and clay cohesion c_u on ultimate capacity. Results show that increasing D significantly improves capacity compared with untreated clay, although the improvement becomes limited beyond a critical thickness D_0. This threshold increases with higher ϕ and decreases with larger c_u. Under eccentric loading, capacity decreases as eccentricity e increases, and a critical value e_0 is identified, beyond which failure is mainly governed by the sand layer. Based on numerical results, design charts are developed for practical evaluation of layered soil foundations over a wide range of D, ϕ, c_u, and e, supporting engineering design and verification of shallow foundations in layered ground conditions.

Key words – Ultimate bearing capacity; Strip footing; Two-layer soils; Centric loading; Eccentric loading; RPFEM.

1. Introduction

The ultimate bearing capacity of strip footings is traditionally estimated using classical solutions developed for homogeneous ground conditions [1]. In reality, natural deposits are typically stratified, reflecting complex geological formation processes rather than ideal uniformity [2]. This discrepancy is particularly important for shallow foundations constructed on soft clay, where inadequate bearing capacity is frequently encountered. To address this limitation, various ground improvement methods have been proposed. Among them, replacing a portion of the upper soft clay with granular material is considered an efficient and cost-effective technique. Such treatment results in a layered system, where a sand layer overlies a relatively weak clay deposit of considerable thickness.

Previous investigations, including limit analysis [3–7] and laboratory testing [8–11], have demonstrated that the performance of strip footings on sand-over-clay systems is governed by both the thickness and strength properties of the sand layer. Reported failure patterns vary, with some mechanisms extending into the underlying clay [12, 13], while others remain restricted within the sand layer [14, 15]. However, the transition between these modes has not been clearly defined in terms of a threshold thickness. Moreover, the quantitative role of the sand internal friction angle remains insufficiently addressed. In addition, most existing studies consider only centrally applied loads, leaving the effect of load eccentricity on layered foundations inadequately explored.

This study examines the bearing capacity and failure characteristics of strip footings placed on a sand layer over weak clay using the Rigid Plastic Finite Element Method (RPFEM). This approach has been widely utilized in ultimate limit state analyses in geotechnical engineering [16–18], showing strong reliability in estimating collapse loads and associated failure patterns [19–21]. The main objective is to clarify the governing mechanisms and quantify the effects of key controlling parameters in layered soil systems. The influence of sand layer thickness, internal friction angle, and load eccentricity is systematically explored.

The findings reveal a critical sand thickness, beyond which failure is confined within the sand layer and the contribution of the underlying clay becomes negligible. The internal friction angle of sand is identified as the primary factor governing improvement in bearing capacity. Furthermore, the effect of load eccentricity is clarified, and a threshold eccentricity is determined at which the failure mechanism resembles that of a homogeneous sandy foundation. Based on these results, design charts from RPFEM are proposed to facilitate practical foundation design on improved layered soils.

2. RPFEM-based analysis of bearing capacity in strip footings

2.1. Soil constitutive model in rigid–plastic analysis

The Tamura et al. [17] rigid–plastic model with a Drucker–Prager yield function is adopted.

$$f(\boldsymbol{\sigma}) = aI_1 + \sqrt{J_2} - b = 0 \quad (1)$$

where, I_1 is the first invariant of the stress tensor σ_{ij}, given by $I_1=tr(\sigma_{ij})$, with tensile stress taken as positive. The second invariant of the deviatoric stress tensor is defined as $J_2 = \frac{1}{2}s_{ij}s_{ij}$. The parameters a and b denote the material constants determined from the soil cohesion (c) and internal friction angle (ϕ) under plane strain conditions. The strain rate $\dot{\varepsilon}$ follows rigid–plastic behavior and satisfies the volumetric constraint related to soil dilatancy.

$$h(\dot{\boldsymbol{\varepsilon}}) = \dot{\varepsilon}_v - \frac{3a}{\sqrt{3a^2+0.5}}\dot{e} = \dot{\varepsilon}_v - \eta\dot{e} = 0 \quad (2)$$

The volumetric and deviatoric strain rates are represented by $\dot{\varepsilon}_v$ and $\dot{e}$, respectively. The parameter η introduced in Eq. (2). The volumetric constraint parameter η does not introduce non-associated behavior. Instead, it controls the admissible relationship between volumetric and deviatoric plastic strain rates within the associated framework. For sand, η governs the dilatancy implied by normality, while for undrained clay it enforces plastic incompressibility. Since collapse load depends on the kinematically admissible plastic flow field, η directly influences the predicted ultimate bearing capacity.

The constitutive formulation proposed by Hoshina et al. [23] incorporates strain-rate effects through a penalty-based approach. Within this framework, the stress–strain rate relation is derived in conjunction with the Drucker–Prager yield criterion and can be written as:

$$\boldsymbol{\sigma} = \frac{b}{\sqrt{3a^2+0.5}}\frac{\dot{\boldsymbol{\varepsilon}}}{\dot{e}} + \kappa\left(\dot{\varepsilon}_v - \eta\dot{e}\right)\left(\boldsymbol{I} - \frac{3a}{\sqrt{3a^2+0.5}}\frac{\dot{\boldsymbol{\varepsilon}}}{\dot{e}}\right) \quad (3)$$

where $\boldsymbol{I}$ denotes the unit tensor, and κ is the penalty parameter. When implemented within a finite element framework, this formulation is consistent with the upper bound theorem in plasticity and corresponds to the RPFEM. A notable feature is that stress evaluation does not require the elastic modulus. For clayey soils, the model can be applied by adopting a Tresca-type yield condition instead of the Drucker–Prager criterion. Under this assumption, the formulation remains applicable to problems involving collapse behavior at the ultimate limit state. Further details regarding rigid body motion can be found in [24-26].

3. Bearing capacity of strip footings under centric loading on sand over clay

3.1. Effect of sand layer thickness on strip footing bearing capacity

The influence of sand layer thickness on the ultimate bearing capacity of a strip footing in a layered soil system is investigated. The model consists of a sand layer, defined by its friction angle ϕ and unit weight γ, placed above a soft clay layer with undrained shear strength c_u. This type of ground profile is frequently observed in practice, where sand replacement is adopted to improve the performance of shallow foundations constructed on weak clay deposits.

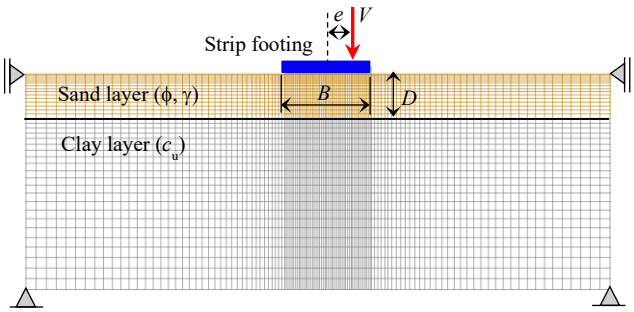

Figure 1. *Boundary condition of strip footing on two-layers using RPFEM*

The numerical model of the strip footing adopted in this study is illustrated in Figure 1. The analysis was carried out using RPFEM under plane strain conditions. The footing, with width B, is located at the surface of the sand layer. The sand thickness is represented by D, while the underlying clay layer is treated as sufficiently deep to avoid any influence of the lower boundary on the failure mechanism. In addition, the computational domain is chosen large enough to reduce boundary effects on the predicted response.

In the numerical analysis, the soil domain is modeled using rigid–plastic finite elements. The base of the model is constrained in both horizontal and vertical directions, whereas the side boundaries are restricted horizontally but remain free vertically. The load eccentricity e is defined as the horizontal offset between the line of action of the vertical load V and the footing centerline. To better represent stress concentration and the associated failure pattern beneath the footing, mesh refinement is applied in the vicinity of the footing base, while a coarser discretization is used away from this region to reduce computational cost. The ultimate bearing capacity is denoted by V. For comparison, $V_{c,max}$ and $V_{s,max}$ correspond to the capacities of footings placed directly on clay and on homogeneous sand, respectively, and are used as reference values to quantify the improvement due to the sand layer.

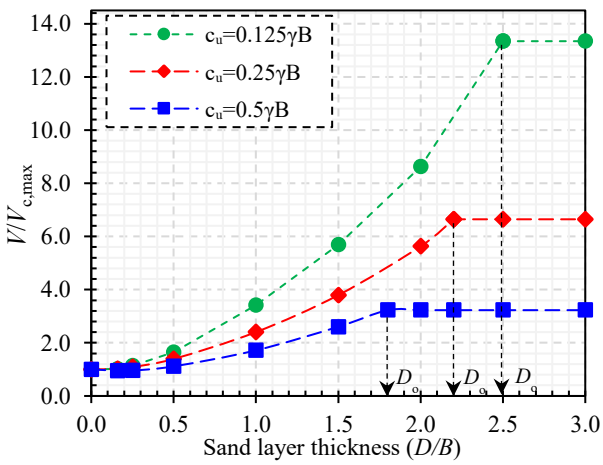

Figure 2. *Effect of sand thickness D on strip footing performance in a sand–clay layered system (sand of ϕ=30°)*

The variation of the normalized bearing capacity ratio $V/V_{c,max}$ with undrained shear strength c_u (0.125–0.5γB) is shown in Figure 2. The ratio $V/V_{c,max}$ represents the improvement in ultimate bearing capacity achieved by introducing a sand layer above the clay deposit. The results indicate that lower values of c_u lead to higher values of $V/V_{c,max}$, demonstrating that the improvement effect of the sand layer becomes more significant when the underlying clay is weaker. As the sand layer thickness D increases, the ratio $V/V_{c,max}$ increases rapidly for small values of D and gradually approaches a constant value at a critical sand layer thickness D_o. The critical thickness depends on the undrained shear strength of the clay layer. Specifically, the present analysis indicates that D_o=2.5B for c_u=0.125γB, D_o=2.25B for c_u=0.25γB, and D_o=1.75B for c_u=0.5γB. When the sand layer thickness exceeds this critical value,

further increases in D have only a negligible influence on the ultimate bearing capacity.

This behavior reflects a progressive change in the governing failure mechanism as the sand layer thickness varies. For relatively small values of sand thickness ($D<D_o$), the failure surface initiates beneath the footing and propagates through the sand layer into the underlying weak clay. In this regime, the response of the system is strongly influenced by the undrained shear strength of the clay, since a significant portion of the failure zone develops within the weaker material. As the thickness of the sand layer increases, the contribution of the sand to the overall shear resistance becomes more pronounced. The failure zone gradually shifts upward, and the extent of penetration into the clay layer decreases. This transition indicates a redistribution of stresses, where the stronger sand layer increasingly governs the load transfer mechanism. When $D\geq D_o$, the failure mechanism becomes fully confined within the sand layer and no longer extends into the underlying clay. As a result, the ultimate bearing capacity is mainly controlled by the shear strength of the sand layer, while the contribution of the underlying clay becomes negligible.

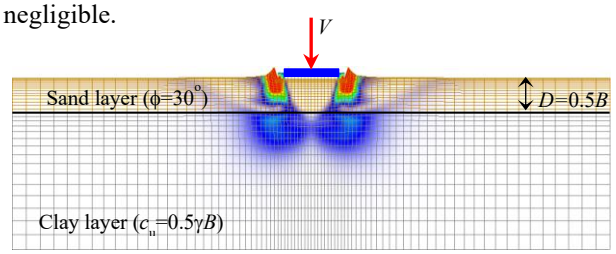

a) Sand layer thickness H=0.5B (V=1329,2 kN/m)

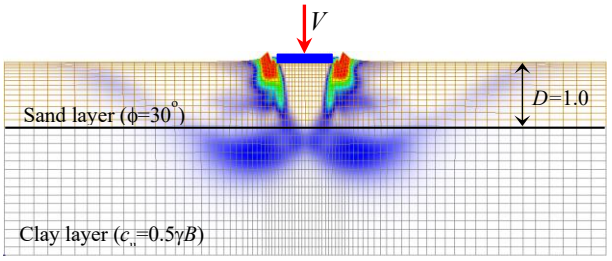

b) Sand layer thickness H=1.0B (V=2011,5 kN/m)

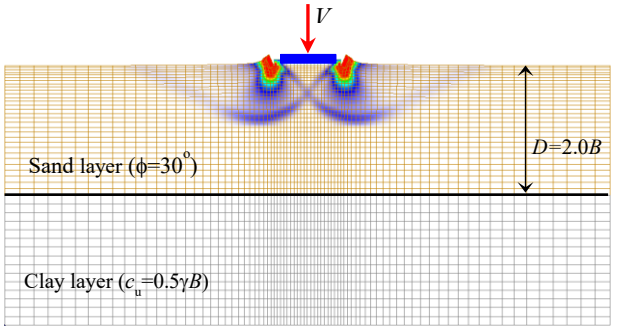

c) Sand layer thickness H=2.0B (V=3793,4 kN/m)

Figure 3. *Variation of failure mechanisms with sand thickness for a centric-loaded strip footing on sand over clay.*

Figure 3 further illustrates the failure mechanisms of the strip footing for sand layer thicknesses D=0.5B, 1.0B, and 2.0B, considering a sand layer with ϕ=30∘ overlying a clay layer with c_u=0.5γB. The results indicate that the failure pattern is strongly influenced by the sand layer thickness. For a thin sand layer (D=0.5B), the failure surface penetrates deeply into the clay layer, indicating that a large portion of plastic energy dissipation occurs within the underlying clay. When the thickness increases to D=1.0B, the failure zone expands within the sand layer but still interacts with the clay, and the plastic dissipation is shared by both soil layers. For a larger thickness (D=2.0B), the failure mechanism becomes fully confined within the sand layer, where most of the plastic energy is dissipated in the stronger granular material, while the contribution of the clay layer becomes negligible. These results indicate that increasing the sand layer thickness modifies both the geometry of the failure surface and the distribution of plastic dissipation, which explains the significant improvement in ultimate bearing capacity observed in the RPFEM analysis.

3.2. Effect of soil shear strength parameters (ϕ and c_u) on strip footing bearing capacity

Replacing the upper portion of a weak soil deposit with a granular layer is a common method to improve the performance of shallow foundations [10]. This study focuses on the effect of the internal friction angle (ϕ) of the sand layer on the bearing capacity of strip footings. An increase in ϕ enhances the shear resistance of the sand, leading to higher bearing capacity. The underlying clay is considered weak to highlight the contribution of the sand layer.

The RPFEM results presented in Figure 4 describe how the normalized capacity ratio $V/V_{c,max}$ varies with the thickness ratio D/B under different combinations of sand friction angle (ϕ=30°, 35°, and 40°) and clay strengths. A clear trend can be observed in which increasing ϕ leads to a substantial enhancement in bearing capacity. This is attributed to the improved shear strength of the sand layer, which allows a larger portion of the applied load to be resisted within the granular material. Consequently, the load transferred to the underlying clay is reduced, and the tendency for deeper failure surfaces is suppressed. The beneficial effect of the sand layer becomes increasingly significant as sand thickness D increases.

The results also show that the critical sand layer thickness D_o, beyond which further increases in D/B produce only marginal improvement in bearing capacity, increases with increasing friction angle. As observed in Figure 5, D_o is approximately in the range of 1.0–2.0B for ϕ=30°, about 1.5–3.0B for ϕ=35°, and may reach up to around 4.0B for ϕ=40°, depending on the cohesion c_u of the clay layer. This trend indicates that increasing the friction angle enhances the ability of the sand layer to distribute stresses more effectively, leading to a more extensive failure zone within the sand. As a result, a greater sand thickness is required to reduce the effect of the underlying weak clay.

The failure mechanisms obtained from the RPFEM analysis are illustrated in Figure 5 for sand friction angles of ϕ=35° and 40°. As ϕ increases, the extent of the failure zone beneath the footing expands both laterally and vertically, indicating an enhanced ability of the sand layer

to mobilize shear strength and distribute the applied load over a larger volume of soil. This effect results in an increase in load-carrying capacity, from V=2458 kN/m for ϕ=35° to V=2856 kN/m for ϕ=40°. Overall, the results highlight the significant influence of the sand strength parameter ϕ on improving the performance of strip footings over weak clay.

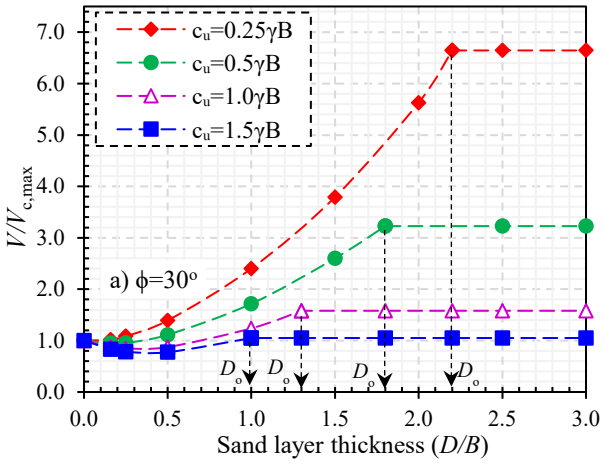

a) Sandy layer (ϕ=30°) over clay layer

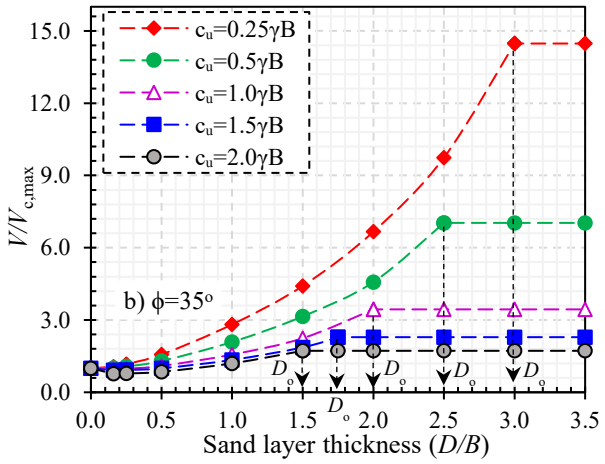

b) Sandy layer (ϕ=35°) over clay layer

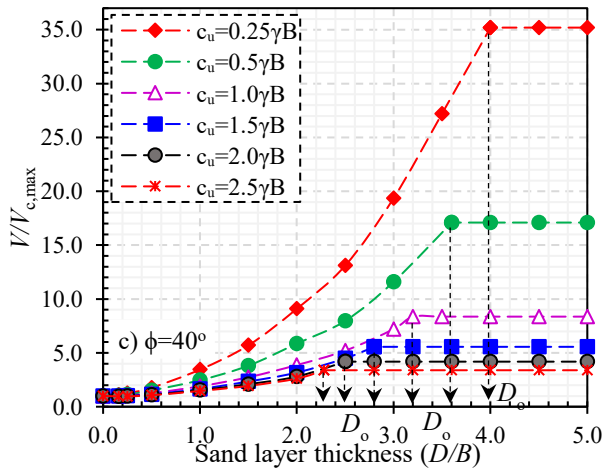

c) Sandy layer (ϕ=40°) over clay layer

Figure 4. *RPFEM-based design chart for the influence of soil shear strength parameters (ϕ and c_u) of two-layered soil on the ultimate bearing capacity of strip footings.*

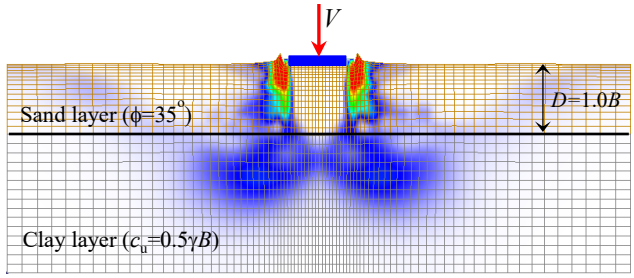

a) sand layer of ϕ=35° (V=2458 kN/m)

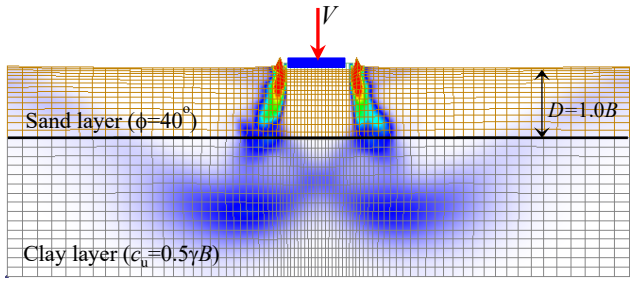

b) sand layer of ϕ=40° (V=2856 kN/m)

Figure 5. *Failure mechanisms of a strip footing over sand-clay layers with increasing sand friction angle (ϕ=35°–40°).*

4. Bearing capacity of strip footings under eccentric loading on sand over clay

To investigate how eccentric loading influences the bearing capacity of strip footings, Figure 6 presents the relationship between the bearing capacity ratio $V/V_{s,max}$ and the eccentricity ratio e/B for sand friction angles ranging from ϕ=30∘ to 40∘ at D/B=1.0. In the case of a homogeneous sand layer, $V/V_{s,max}$ decreases in a nonlinear manner as the eccentricity ratio increases. This reduction is attributed to the effective narrowing of the footing width and the formation of stress concentrations near the edge of the footing under off-center loading. The computed results for single-layer sand show good agreement with the predictions reported by Meyerhof [27].

A different trend is observed for the sand-over-clay system presented in Figure 6. The normalized bearing capacity ratio $V/V_{s,max}$ shows an approximately linear decrease with increasing eccentricity ratio e/B, even at relatively low eccentricities. This behavior indicates that both the sand layer and the underlying clay layer participate in the failure mechanism and contribute to load resistance. However, as the eccentricity increases to a certain level, the normalized bearing capacity of the layered system approaches that of a uniform sand deposit. For c_u=1.0γB, the critical eccentricity ratio e_o is about 0.1B for ϕ=30∘, 0.2B for ϕ=35∘, and 0.33B for ϕ=40∘. When this limit is exceeded, the bearing response becomes comparable to that of single-layer sand, suggesting that the failure zone is largely restricted to the sand layer, while the contribution from the clay layer becomes negligible.

The results indicate a gradual change in the dominant failure mechaism as the load eccentricity increases. For small eccentricities, the stress beneath the footing is distributed in a relatively uniform manner, enabling both the sand layer and the underlying clay to contribute to load resistance. With increasing eccentricity, stresses tend to

concentrate toward the loaded side of the footing, and the deformation zone progressively develops within the upper sand layer. Once the eccentricity exceeds a critical threshold e_o, the shear zone is largely restricted to the sand layer, and the influence of the clay layer becomes negligible. Under this condition, the layered soil system responds similarly to a single-layer sand deposit.

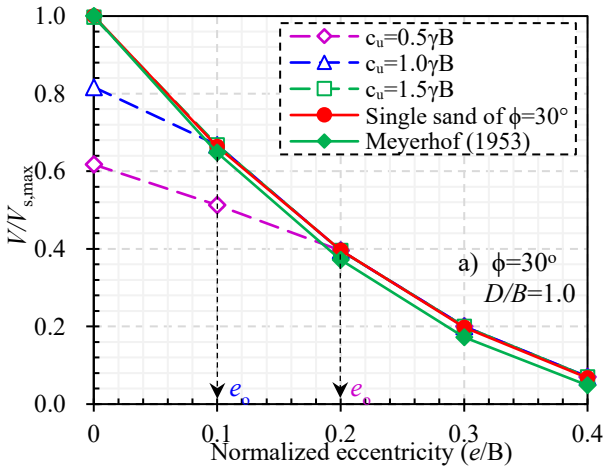

a) Sandy layer (ϕ=30°) over clay layer

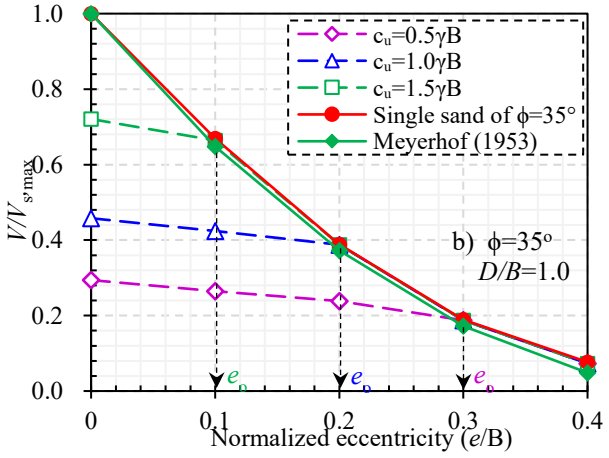

b) Sandy layer (ϕ=35°) over clay layer

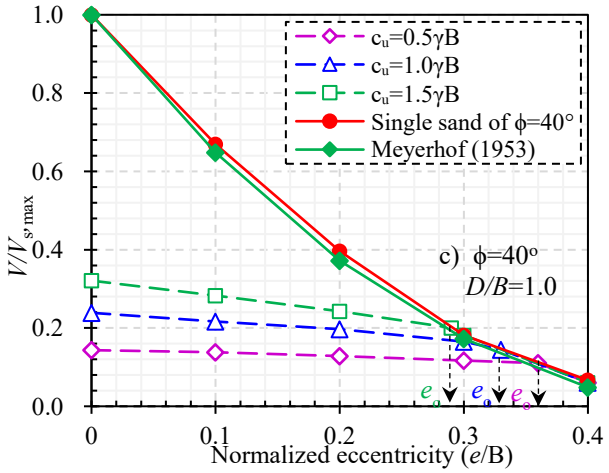

c) Sandy layer (ϕ=40°) over clay layer

Figure 6. *RPFEM-based design chart for the influence of eccentric loads on ultimate bearing capacity $V/V_{s,max}$ of strip footing in case of D/B=1.0*

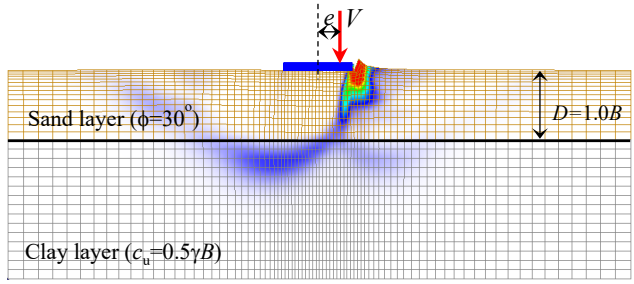

a) Eccentric length e=0.1B (V=1874 kN/m)

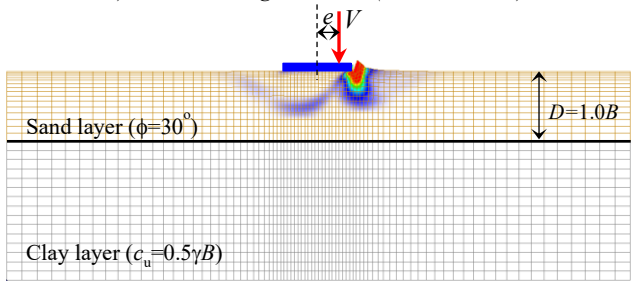

b) Eccentric length e=0.2B (V=1557 kN/m)

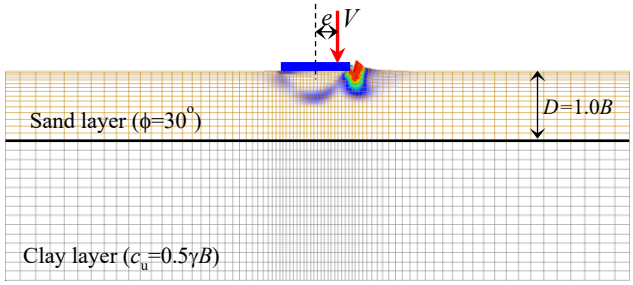

c) Eccentric length e=0.3B (V=816 kN/m)

Figure 7. *Failure mechanisms of an eccentric-loaded footing on sand ϕ=30° over clay c_u=0.5γB*

Figure 7 demonstrates the change in failure characteristics as the load eccentricity increases. The computed deformation fields beneath the strip footing are presented for various values of *e/B*, where a sand layer with ϕ=30∘ overlies a clay layer defined by c_u=0.5γB at *D/B*=1.0. For a small eccentricity (*e*=0.1*B*), the failure region develops across both soil layers, suggesting that the bearing response is controlled by the interaction between the sand and the underlying clay. With increasing eccentricity, the stress field shifts toward the loaded side, leading to a more localized deformation zone within the upper sand layer. At a higher eccentricity (*e*=0.3*B*), the failure region is predominantly contained within the sand layer, and the contribution from the clay layer becomes insignificant. This shift in behavior is associated with a pronounced decrease in the ultimate bearing capacity, from *V*=1874kN/m at *e*=0.1*B* to *V*=816 kN/m at *e*=0.3*B*. The reduction can be explained by the combined effect of a smaller effective load-transfer width and the increasing concentration of stresses near the loaded edge under eccentric loading.

Overall, The RPFEM analysis demonstrates that load eccentricity has a significant influence on both the bearing capacity and the associated failure behavior of strip footings on layered soils. In particular, increasing eccentricity not only leads to a reduction in bearing capacity but also modifies the governing failure pattern of strip footings.

5. Conclusion

The main findings are summarized as follows:

(1) The ultimate bearing capacity of strip footings resting on sand-over-clay systems increases significantly with increasing sand layer thickness. However, this increase becomes negligible beyond a critical sand thickness D_o, which depends on the undrained shear strength of the underlying clay. The present RPFEM results indicate that D_o is approximately 2.5B, 2.25B, and 1.75B for c_u=0.125γB, 0.25γB, and 0.5γB with ϕ=30°, respectively, for which RPFEM-based design charts are provided to facilitate practical design.

(2) The improvement in bearing capacity is governed primarily by the internal friction angle ϕ of the sand layer. Higher friction angles lead to significantly larger increases in bearing capacity, indicating that the sand layer becomes the dominant load-resisting medium once the sand thickness exceeds the critical value.

(3) Under eccentric loading, the ultimate bearing capacity decreases with increasing eccentricity due to the reduction in effective footing width and stress concentration near the loaded edge. A critical eccentricity e_o is identified, beyond which the bearing capacity of the sand–clay system converges to that of a homogeneous sandy soil, and the corresponding RPFEM-based design charts are also provided for engineering applications.

(4) The RPFEM simulations clearly reveal the transition of failure mechanisms in layered soils. For small sand thicknesses or small eccentricities, the failure zone extends into both the sand and clay layers, and the bearing capacity is controlled by the combined resistance of the two layers. As the sand thickness increases or the eccentricity becomes larger, the failure mechanism progressively shifts upward and eventually develops entirely within the sand layer.

Overall, the RPFEM results clearly capture the effects of soil layering, sand shear strength, and load eccentricity on bearing capacity and failure mechanisms. The findings provide useful and practical guidance for the design of strip footings on layered soils improved by sand replacement.

REFERENCES

[1] K. Terzaghi and R. B. Peck, *Soil Mechanics in Engineering Practice*, John Wiley and Sons, New York, 1948.

[2] H. J. Burd and S. Frydman, "Bearing capacity of plane-strain footings on layered soils", *Canadian Geotechnical Journal*, vol. 34, no. 2, pp. 241–253, 1997.

[3] M. Huang and H. L. Qin, "Upper-bound multi-rigid-block solutions for bearing capacity of two-layered soils", *Computers and Geotechnics*, vol. 36, no. 3, pp. 525–529, 2009.

[4] G. Qiu and J. Grabe, "Numerical investigation of bearing capacity due to spudcan penetration in sand overlying clay", *Canadian Geotechnical Journal*, vol. 49, no. 12, pp. 1393–1407, 2012.

[5] A. Rajaei, A. Keshavarz, and A. Ghahramani, "Static and seismic bearing capacity of strip footings on sand overlying clay soils", *Iranian Journal of Science and Technology, Transactions of Civil Engineering*, vol. 43, no. 1, pp. 69–80, 2019.

[6] G. Zheng, E. Wang, J. Zhao, H. Zhou, and D. Nie, "Ultimate bearing capacity of vertically loaded strip footings on sand overlying clay", *Computers and Geotechnics*, vol. 115, 103151, 2019.

[7] S. Salimi Eshkevari, A. J. Abbo, and G. Kouretzis, "Bearing capacity of strip footings on sand over clay", *Canadian Geotechnical Journal*, vol. 56, no. 5, pp. 699–709, 2019.

[8] W. H. Craig and K. Chua, "Deep penetration of spud-can foundations on sand and clay", *Géotechnique*, vol. 40, no. 4, pp. 541–556, 1990.

[9] M. Okamura, J. Takemura, and T. Kimura, "Centrifuge model tests on bearing capacity and deformation of sand layer overlying clay", *Soils and Foundations*, vol. 37, no. 1, pp. 73–88, 1997.

[10] K. L. Teh and C. F. Leung, "Centrifuge model study of spudcan penetration in sand overlying clay", *Géotechnique*, vol. 60, no. 11, pp. 825–842, 2010.

[11] M. S. Hossain, Y. Hu, and D. Ekaputra, "Skirted foundation to mitigate spudcan punch-through on sand-over-clay", *Géotechnique*, vol. 64, no. 4, pp. 333–340, 2014.

[12] J. D. Brown and W. G. Paterson, "Failure of an oil storage tank founded on a sensitive marine clay", *Canadian Geotechnical Journal*, vol. 1, no. 4, pp. 205–214, 1964.

[13] A. S. Vesic, "Analysis of ultimate loads of shallow foundations", *Journal of the Soil Mechanics and Foundations Division (ASCE)*, vol. 99, no. 1, pp. 45–73, 1973.

[14] F. Yang, X. C. Zheng, L. H. Zhao, and Y. G. Tan, "Ultimate bearing capacity of a strip footing placed on sand with a rigid basement", *Computers and Geotechnics*, vol. 77, pp. 115–119, 2016.

[15] L. Rahimi, N. Ganjian, and H. Azizian, "New algorithm to estimate the bearing capacity of two cohesive-frictional layered soil", *Iranian Journal of Science and Technology, Transactions of Civil Engineering,* vol. 49, no. 2, pp. 1901–1914, 2025.

[16] T. Tamura, S. Kobayashi, and T. Sumi, "Limit analysis of soil structure by rigid plastic finite element method", *Soils and Foundations*, vol. 24, no. 1, pp. 34–42, 1984.

[17] T. Tamura, S. Kobayashi, and T. Sumi, "Rigid plastic finite element method for frictional materials", *Soils and Foundations*, vol. 27, no. 3, pp. 1–12, 1987.

[18] T. Tamura, S. Kobayashi, and T. Sumi, "Rigid plastic finite element method in geotechnical engineering", *Current Japanese Material Research*, pp. 15–23, 1990.

[19] P. N. Quang. "Estimation of Ultimate Lateral Resistance of Pile Group, and Ultimate Bearing Capacity of Rigid Footing under Complex Load by using Rigid Plastic Finite Element Method", 2020. (Doctoral dissertation, Nagaoka University of Technology)

[20] P. N. Quang, S. Ohtsuka, K. Isobe, and Y. Fukumoto, "Consideration on Limit Load Space of Footing on Various Soils Under Eccentric Vertical Load", In *Challenges and Innovations in Geomechanics: Proceedings of the 16th International Conference of IACMAG-Volume 2 16*, 2021, pp. 75-84.

[21] P. N. Quang, and S. Ohtsuka, "Numerical Investigation on Bearing Capacity of Rigid Footing on Sandy Soils Under Eccentrically Inclined Load", In *Proceedings of the 2nd Vietnam Symposium on Advances in Offshore Engineering: Sustainable Energy and Marine Planning*. Springer Singapore, 2022, pp. 333-341.

[22] T. Hoshina, "Rigid plastic stability analysis for slope including thin weak layer", *Japanese Geotechnical Journal*, vol. 6, no. 2, pp. 191-200, 2011.

[23] T. Hoshina, S. Ohtsuka, and K. Isobe, "Ultimate bearing capacity of ground by Rigid plastic finite element method taking account of stress dependent non-linear strength property", *Journal of Applied Mechanics*, vol. 6, no. 2, pp. I_327-I_336, 2012.

[24] P. N. Quang, S. Ohtsuka, K. Isobe, N. V. Pham, and P. H. Hoa, "Undrained failure envelope (*V–H–M*) of rigid strip footings on clayey soil slopes under eccentric and inclined loads," *Arabian Journal for Science and Engineering*, pp. 1–28, 2025.

[25] N. Q. Pham and N. V. Pham, "Undrained bearing capacity of shallow foundations on clay slopes under eccentric loading using a no-tensile strength analysis," *International Journal of Civil Engineering*, pp. 1–21, 2025.

[26] N. Q. Pham and N. V. Pham, "Effect of Footing Roughness on Ultimate Bearing Capacity of Rigid Strip Footing on Sandy Soil Slope". *The University of Danang - Journal of Science and Technology*, vol. 21, no. 12.1, pp. 22-27, 2023, doi:10.31130/ud-jst.2023.472E

[27] G. G. Meyerhof, "The bearing capacity of foundations under eccentric and inclined loads," *Proceedings of the 3rd International Conference on Soil Mechanics and Foundation Engineering*, vol. 1, pp. 440–445, 1953.